Comparison between Voltage Oriented Control and Synchronous Power Control for Grid-Connected Inverter Applications

R. Miceli, C. Nevoloso, G. Scaglione, G. Schettino, G. Sorrentino and F. Viola
Department of Engineering
University of Palermo
Viale delle scienze, building 9, 90128, Palermo, (*Italy*)

***Abstract*—With the rising of renewable power generation, there are new challenges to be addressed in order to maintain the electrical system operation stability. So, in literature, new grid-connected inverter control techniques have been studied. This paper focuses on a comparison between a grid-following control technique, called Voltage Oriented Control and a grid-forming control technique, called Synchronous Power Control, to underline the advantages offered by the latter. Through a simulation analysis in Matlab/Simulink environment, the benefits and drawbacks of these control approaches have been analyzed and discussed.**

***Index Terms*—Inertia, Phase-Locked Loop, Synchronous Power Control, Voltage Oriented Control.**

I. Introduction

Renewable energy sources are fundamental to achieve the electrical system decarbonization. According to [1]-[4], these new ways to produce electrical energy require innovative solutions to overcome the operative limits due to the sources aleatority. As these power plants substitute the traditional ones, electrical system operation becomes more challenging.

In particular, the major challenges are frequency and voltage regulation [5]. This is because, as of today, most renewable energy sources inverters are controlled by a technique called grid-following control where the inverter is controlled to inject the maximum amount of active power available without caring for frequency or voltage regulation. Thus, in this case, they can't provide inertia to the grid [6].

Inertia is a fundamental characteristic of traditional synchronous generators. Since they are rotational machines, they are able to store rotational kinetic energy. This feature is very important for the electrical system frequency dynamics and stability because it helps by reducing the frequency deviations caused by power imbalances [7].

To face these new challenges, new control strategies have been developed in literature, which are called grid-forming or grid-supporting control techniques. In this case, the main objective of the inverter control is to provide active power injection for frequency regulation and reactive power injection for voltage regulation to offer grid support. In some cases, these techniques can also provide inertia to the grid [6].

There are several grid-forming techniques that can be classified as follows [6]:

- Droop control;
- Synchronous machine-based control;
- Other control types.

Droop control techniques are based on the same principle of the synchronous machine governors. The main disadvantage of these techniques is that they cannot provide inertia to the grid.

Synchronous machine-based control techniques are based on the emulation of a traditional synchronous generator and have the advantage of being able to provide inertia to the grid.

Other control types are a set of non-linear techniques that don't belong to the two previous categories [6].

The grid-forming technique taken into consideration falls into the Synchronous machine-based control and, in particular, it is a Virtual Synchronous Generator control technique that uses the virtual admittance block instead of the virtual impedance block for the inner control loop [8]. The concept of the Virtual Synchronous Generator was first introduced in [9].

In this paper, a comparison between Voltage Oriented Control [10] and Synchronous Power Control [11] has been conducted. In detail, an extensive simulation analysis has been carried out on Matlab/Simulink environment for performance comparison purposes by considering frequency and voltage disturbances.

The rest of this paper is organized as follows. Section II presents the system taken into consideration; Section III describes the control system tuning; Section IV describes the software implementation; Section V provides simulation results; finally, Section VI summarizes the conclusion of the work.

II. System description

This section describes the system considered for comparison purposes. The system consists of a three-phase grid-connected inverter, where a constant DC voltage has been considered, and a grid LCL-filter. It was necessary to connect and design a filter between the inverter and the grid in order to reduce the harmonic content produced by

the converter. The simulation analysis has been carried out by considering the system under test connected to the three-phase low voltage grid and the system parameters are shown in TABLE I.

TABLE I
SYSTEM PARAMETERS [11]

DC-link voltage	700 V
Switching frequency	10 kHz
Rated power	10 kW
Grid phase-to-phase voltage (*RMS*)	400 V
Grid rated frequency	50 Hz

In the follow a brief description of the system under test.

A. Inverter

The inverter used is a three-phase Voltage Source Inverter (VSI) based on the power MOSFET. The modulation strategy used is Sinusoidal Pulse Width Modulation (SPWM) strategy.
A simplified scheme of the inverter is depicted in Fig. 1.

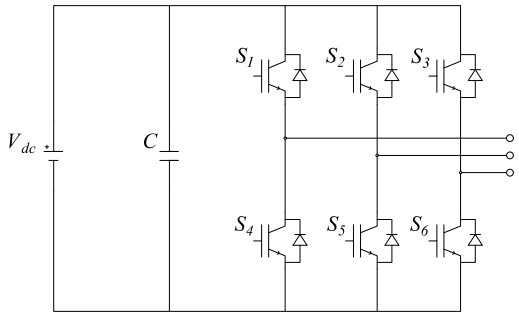

Fig. 1. Simplified three-phase VSI inverter scheme.

This inverter type was taken into consideration because it is the most used and commercially diffused for this type of application.

B. LCL Filter

The type of filter used is the LCL filter which is one of the most used for grid-connected applications.
A scheme of the grid-connected inverter comprehending the filter is depicted in Fig. 2.

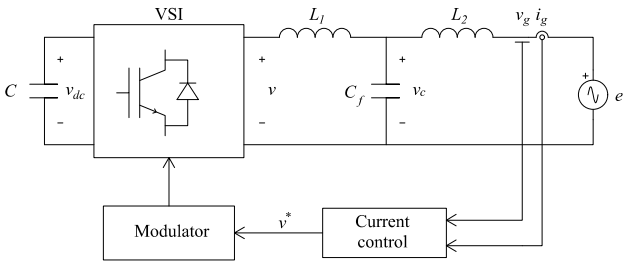

Fig. 2. Grid-connected inverter scheme.

The filter was designed according to [12]. The filter capacitor design is based on the definition of the base impedance. From it, the base capacitor value is derived. Based on its value, the filter capacitor is chosen by limiting the reactive power absorption of the filter that was fixed at 5% of the rated power.

The converter-side inductance is chosen based on the desired maximum current ripple. In this work, it was chosen a maximum current ripple equal to 10% of the converter current peak value. The grid-side inductance is chosen based on the value of the converter-side inductance and by considering a reduction factor equal to 0,2.
The damping resistance is chosen taking into consideration the resonance frequency.
The main filter features obtained by the design study are reported in TABLE II.

TABLE II
FILTER DESIGN VALUES

Converter-side inductance, L_1	5,7 mH
Converter-side inductance resistance, r_1	0,01 Ω
Grid-side inductance, L_2	0,152 mH
Grid-side inductance resistance, r_2	0,01 Ω
Capacitance, C_f	9,94 μF
Damping resistance, R_d	1,289 Ω

C. Voltage Oriented Control

The grid-following control technique considered in this paper is called Voltage Oriented Control and it works in a *dq* rotating reference frame to allow the use of PI regulators. The synchronization to the grid is achieved by the alignment between the *d*-axis component of the inverter output voltage v_d and the *d*-axis component of the grid voltage v_{gd}, hence the name Voltage Oriented Control. The control scheme of this control is depicted in Fig. 3. As shown in this control scheme has two control loops, one for the *d*-axis inverter output current component i_d and one for the *q*-axis inverter output current component i_q.

There are also feed-forward terms to decouple the equations and achieve better dynamic performance.

D. Synchronous Power Control

The grid-forming control technique considered in this paper is called Synchronous Power Control and it's based on the emulation of a synchronous machine. It can provide inertia and has the advantage that the active power response parameters, such as the inertia constant H, the damping coefficient ζ and the droop coefficient D_P can be assigned independently from each other.

Grid synchronization is achieved by the active power exchange between the inverter and the grid.
The control scheme of this control is depicted in Fig. 4. This control has two outer control loops. One is for active power control. From this loop, it is derived the inverter output frequency ω. The other outer control loop is for reactive power control and it consists of a simple PI regulator. The output of this loop is the magnitude of the virtual emf e of the emulated synchronous machine.

The inverter output frequency ω and the virtual emf magnitude E are sent to a Voltage Controlled Oscillator (VCO) in which virtual emf sinewave is generated. In particular, the virtual emf phase value is obtained by integrating the output frequency ω. Then, the virtual emf e minus the voltage grid v goes into the Virtual Admittance block which emulates the synchronous generator output reactance.

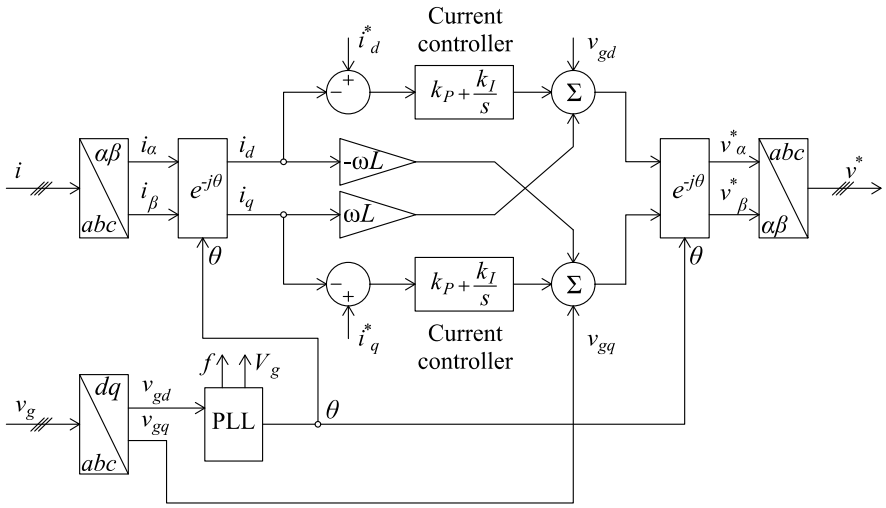

Fig. 3. Voltage Oriented Control Scheme.

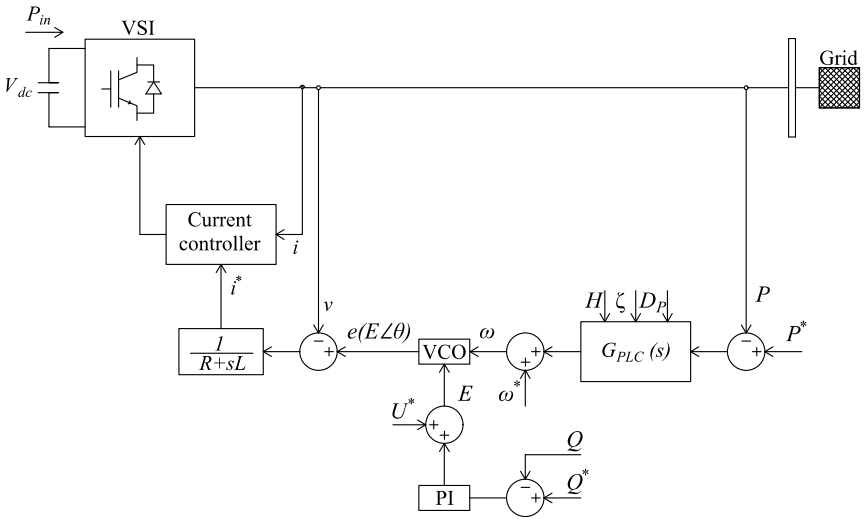

Fig. 4. Synchronous Power Control scheme.

The output of this block is the reference current i^* which goes to the current controller of the inverter.

This control scheme has several advantages, such as the direct current control, the virtual admittance block and the fact that it doesn't require a Phase-Locked Loop algorithm to achieve grid synchronization.

III. Control System Tuning

The Synchronous Power Control shares the same current control of the Voltage Oriented Control, so the two current PI controllers are tuned in the same way.

A. Voltage Oriented Control

In order to tune the two current PI regulators, it is considered the control scheme depicted in Fig. 5.

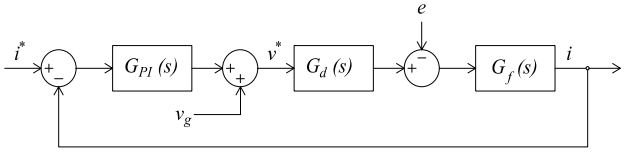

Fig. 5. Current control scheme.

As shown in Fig.5, the control scheme is composed by three transfer function: $G_{PI}(s)$ is the transfer function of the PI regulator (1), $G_d(s)$ is the transfer function of the inverter (2), $G_f(s)$ is the transfer function of the LCL filter (3);

$$G_{PI}(s) = K_P + \frac{K_I}{s} = K_P\left(1 + \frac{1}{T_I s}\right) \tag{1}$$

$$G_d(s) = \frac{1}{1 + 1.5T_s s} \tag{2}$$

$$G_f(s) = \frac{1}{R + Ls} \tag{3}$$

where T_s is the switching period, R and L are the total LCL filter resistance and inductance, K_P and T_I are the PI regulator proportional gain and integral constant, respectively. In detail, in the transfer function of the LCL filter has been neglected the presence of the capacitor branch.

Considering this control scheme, the closed loop transfer function is the following:

$$W(s)=\frac{\frac{1}{R}(T_I s+1)K_P}{\left(\frac{L}{R}s+1\right)(1.5T_s s+1)T_I s+\frac{1}{R}(T_I s+1)K_P}. \quad (4)$$

Then, by choosing the integral time constant equal to:

$$T_I=\frac{L}{R} \quad (5)$$

a zero-pole cancellation is realized, so the closed loop transfer function becomes:

$$W(s)=\frac{\frac{K_P}{R}}{s\frac{L}{R}(1.5T_s s+1)+\frac{K_P}{R}} \quad (6)$$

By expressing (4) in the typical second-order system form:

$$W(s)=\frac{{\omega_n}^2}{s^2+2\xi\omega_n s+{\omega_n}^2} \quad (7)$$

where:

$$\omega_n=\sqrt{\frac{K_P}{L1.5T_s}} \quad (8)$$

$$\xi=\frac{1}{3T_s\omega_n} \quad (9)$$

Assigning ξ, ω_n is evaluated by equation (9) so the proportional gain is chosen according to (8):

$$K_P=L1.5T_s{\omega_n}^2 \quad (10)$$

B. Synchronous Power Control

The tuning of the active power control loop is aimed to assign the desired values of virtual inertia H, damping coefficient ζ and droop coefficient D_P by choosing the gains of the active power transfer function, K_I, K_G and K_P. The active power control loop can be modelled according to Fig. 6.

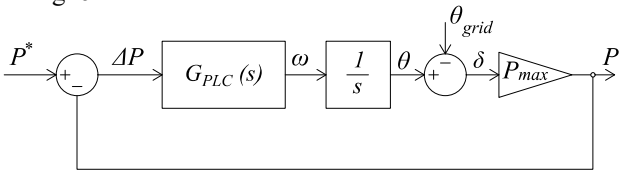

Fig. 6. Active Power control loop.

The scheme of the active power loop transfer function is depicted in Fig. 7.

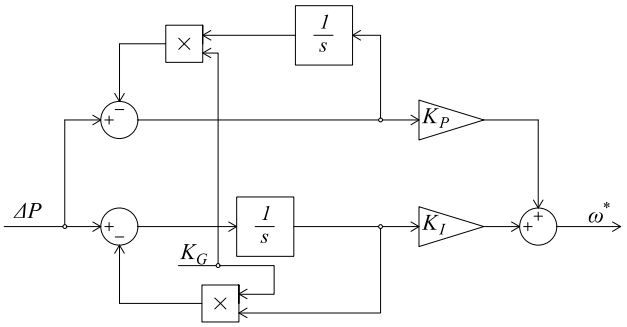

Fig. 7. Active power loop transfer function.

The active power control loop transfer function of Fig. 7 is:

$$G_{PLC}(s)=\frac{K_P s+K_I}{s+K_G} \quad (11)$$

Considering the scheme shown in Fig. 6 and the transfer function of Fig. 7, the active power control loop transfer function of Fig. 6 can be expressed as:

$$\frac{P}{P^*}(s)=\frac{(2\xi\omega_n-K_G)s+{\omega_n}^2}{s^2+2\xi\omega_n s+{\omega_n}^2} \quad (12)$$

where:

$$\xi=\frac{P_{max}K_P+K_G}{2\omega_n} \quad (13)$$

$$\omega_n=\sqrt{P_{max}K_I} \quad (14)$$

P_{max} is the admittance gain defined in [11].
Considering the synchronous machine swing equation, ω_n can be also expressed as:

$$\omega_n=\sqrt{\frac{P_{max}\omega_s}{2S_N H}} \quad (15)$$

By assigning the desired value of inertia constant H, ω_n can be evaluated from the equation (15).
Substituting ω_n in the equation (14), K_I can be set equal to:

$$K_I=\frac{{\omega_n}^2}{P_{max}} \quad (16)$$

Then, by assigning D_P, K_G can be set equal to:

$$K_G=\frac{1000K_I D_P}{2\pi P_{max}} \quad (17)$$

Finally, by assigning ζ, K_P can be set equal to:

$$K_P=\frac{2\omega_n\xi-K_G}{P_{max}} \quad (18)$$

IV. Software Implementation

The software implementation has been carried out in Matlab/Simulink environment.

In particular, the Specialized Power System Simulink library was used in order to build the model. The model consists of the control subsystem, the inverter model, the switches control subsystem, the LCL filter model, the grid model and the subsystem that performs the required coordinates transformations. The inverter model was built using MOSFET blocks of the specified library. Moreover, it was built a logic circuit to avoid the short circuit of a leg of the inverter. The LCL filter was built using the series RLC load blocks. The grid model was built differently for the two control techniques as described later.

A. *Voltage Oriented Control*

In order to simulate the control system of Fig. 3 coordinates transformation from the three-phase domain into the *dq0* synchronous reference frame have been used [10]. The three output voltages v^* of the control scheme of Fig. 3 are the three modulating signals of the inverter PWM. The grid model was built by three wye-connected ideal AC voltage sources. The two current reference values are obtained by setting the desired values of injected active and reactive power.

B. *Synchronous Power Control*

The Simulink model of this type of control is almost the same as the previous one but with the following differences.

It has a new Subsystem for the VSG control, which recreates the control scheme of Fig. 4, in order to obtain the current reference values. It doesn't have a Phase Locked Loop block. It has a slightly modified grid model to change grid frequency and voltage. Moreover, a reactive power droop control was added to change the reactive power reference according to the grid voltage variations.

V. Simulation Results

In order to underline the differences between these two types of control several simulations have been conducted. In detail, in order to achieve a detailed comparison, the simulation analysis has been subdivided in three parts. The first analysis shows the Voltage Oriented Control performance when the maximum active power is provided to the ideal grid. The second analysis shows the Synchronous Power Control performance when the maximum active power is provided and some frequency and voltage grid variations occur. Finally, the third one was based on the comparison between the two control techniques in terms of grid synchronization under grid voltage disturbances.

A. *Voltage Oriented Control*

The active power reference was set equal to 10 kW. The reactive power reference was set equal to 0 kVAR. Grid frequency and voltage were maintained equal to their nominal values.

From Fig. 8 and Fig. 9, it can be observed that this type of control is very fast and it doesn't provide inertia to the grid.

Also, from Fig. 10 it can be observed that the LCL filter is able to reduce the grid side current harmonics below the limits specified in the IEEE Std 1547-2018.

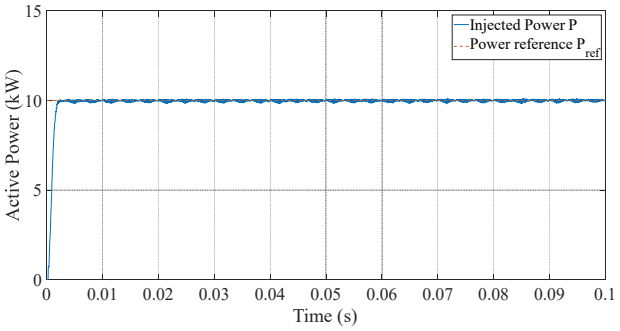

Fig. 8. Comparison between the inverter injected active power with the respective reference.

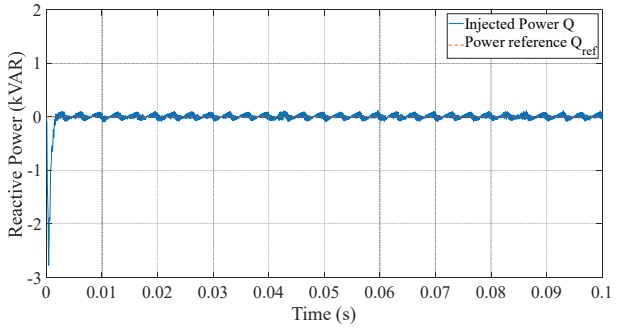

Fig. 9. Comparison between the inverter injected reactive power with the respective reference.

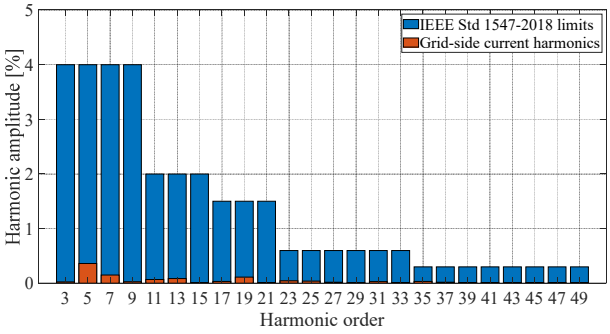

Fig. 10. Comparison between the IEEE Std 1547-2018 limits and the Grid-side current harmonics.

B. *Synchronous Power Control*

The active power reference was set equal to 6 kW and the reactive power reference was set equal to 0 kVAR as shown in Fig. 11 and Fig. 12. The virtual inertia value H was set equal to 10 s. The active power droop coefficient D_P was set equal to 2 kW/Hz.

To highlight the grid-supporting features of this control two kinds of disturbances have been simulated. In particular, to underline the active power support contribution a grid frequency drop of 0,1 Hz has been simulated between time instants 2s and 2,5s.

During this time, it can be observed that the inverter injects a higher value of active power in order to face this grid frequency drop. To underline the reactive power support contribution a 3% grid voltage drop has been simulated between time instants 5s and 6s. During this time, we can observe that the inverter is able to inject negative reactive power to face this voltage grid drop. Moreover, from Fig. 11 it can be observed that the active

power response is slow. This is because this control technique takes into account a virtual inertia.

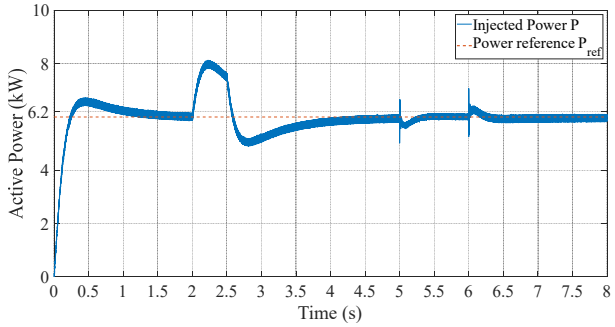

Fig. 11. Comparison between the inverter injected active power with the respective reference.

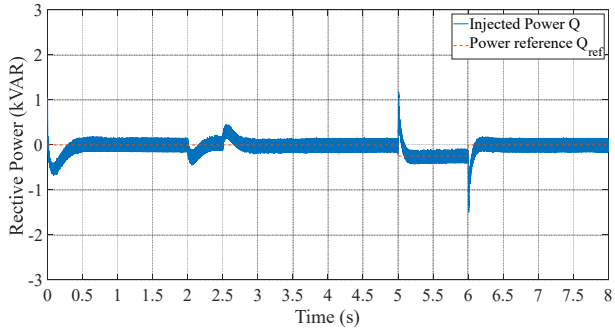

Fig. 12. Comparison between the inverter injected reactive power with the respective reference.

C. *Synchronization capability comparison*

In order to test the synchronization capability of the two control techniques a 5th harmonic injection on the grid voltage has been simulated, as depicted in Fig. 13.

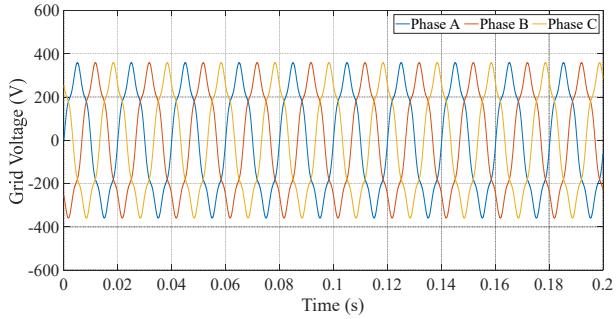

Fig. 13. Voltage grid.

Moreover, a 0.2 Hz grid frequency permanent drop has been simulated. From Fig. 14 it can be observed that the grid-following control technique fails to synchronize to the grid because there are high amplitude oscillations of the output inverter frequency around the grid frequency. This is due to the use of the Phase-Locked Loop synchronization algorithm which uses a PI regulator in order to align the d-axis inverter voltage component to the d-axis grid voltage component to achieve grid synchronization.

Looking at Fig. 15, it can be observed that the grid-forming technique, is able to synchronize with the grid despite the grid-voltage disturbance because acts in a different way, that is it achieves grid synchronization by exchanging active power with the grid, as a traditional synchronous generator would do.

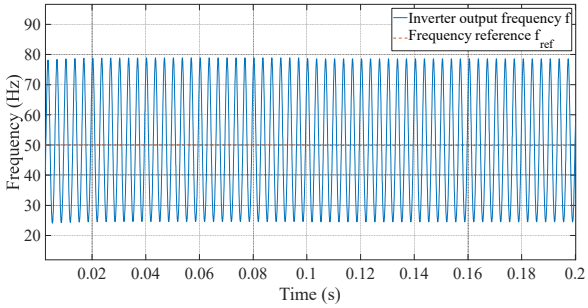

Fig. 14. Comparison between the inverter output frequency with the respective reference (grid-following).

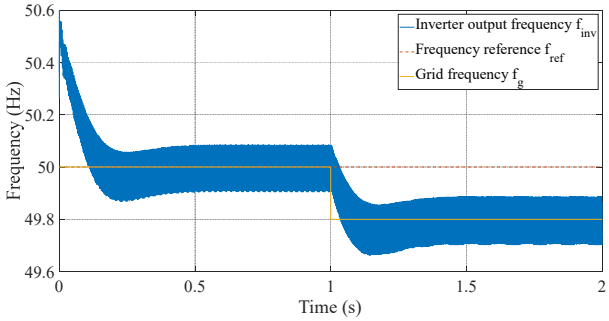

Fig. 15. Comparison between the inverter output frequency with the respective reference and the grid frequency (grid-forming).

VI. Conclusion

In this paper, a comparison between Voltage Oriented Control and Synchronous Power Control has been studied and analyzed. It was observed that the grid-forming control technique is able to provide inertia to the grid. Moreover, it can inject active and reactive power into the grid to support the grid in case of frequency and voltage variations. Finally, in order to analyze the synchronization capability of the two control techniques, a 5th harmonic injection into the voltage grid has been considered and simulated. It can be observed that the grid-forming technique is still able to synchronize to the grid.

ACKNOWLEDGEMENT

This work was supported in part by the Prin 2017-Settore/Ambito di intervento: PE7 linea C Advanced power-trains and -systems for full electric aircrafts under Grant 2017MS9F49, in part by the Sustainable Mobility Center (Centro Nazionale per la Mobilità Sostenibile—CNMS) under Grant CN00000023 CUP B73C22000760001 and by the Network 4 Energy Sustainable Transition (NEST) ID number PE0000021 CUP B73C22001280006.

References

[1] M. Busu, ‘‘The role of renewables in a low-carbon society: Evidence from a multivariate panel data analysis at the EU level,’’ Sustainability, vol. 11, no. 19, p. 5260, Sep. 2019.

[2] M. Caruso, A. O. Di Tommaso, F. Genduso and R. Miceli, "Experimental investigation on high efficiency real-time control algorithms for IPMSMs," 2014 International Conference on Renewable Energy Research and

Application (ICRERA), Milwaukee, WI, USA, 2014, pp. 974-979, doi: 10.1109/ICRERA.2014.7016531.

[3] V. Di Dio, R. Miceli, C. Rando and G. Zizzo, "Dynamics photovoltaic generators: Technical aspects and economical valuation," SPEEDAM 2010, Pisa, Italy, 2010, pp. 635-640, doi: 10.1109/SPEEDAM.2010.5542261.

[4] V. Di Dio, D. La Cascia, R. Liga and R. Miceli, "Integrated mathematical model of proton exchange membrane fuel cell stack (PEMFC) with automotive synchronous electrical power drive," 2008 18th International Conference on Electrical Machines, Vilamoura, Portugal, 2008, pp. 1-6, doi: 10.1109/ICELMACH.2008.4800045.

[5] Y. Lin, J. H. Eto, B. B. Johnson, J. D. Flicker, R. H. Lasseter, H. N. V. Pico, G.-S. Seo, B. J. Pierre, and A. Ellis, ‘‘Research roadmap on grid-forming inverters,’’ Nat. Renew. Energy Lab., Golden, CO, USA, Tech. Rep. NREL/TP-5D00-73476, 2020.

[6] D. B. Rathnayake et al., "Grid Forming Inverter Modeling, Control, and Applications," in IEEE Access, vol. 9, pp. 114781-114807, 2021, doi: 10.1109/ACCESS.2021.3104617.

[7] Ulbig, Andreas & Borsche, Theodor & Andersson, Göran. (2013). Impact of Low Rotational Inertia on Power System Stability and Operation. IFAC Proceedings Volumes (IFAC-PapersOnline). 19.

[8] P. Rodriguez, I. Candela, C. Citro, J. Rocabert, and A. Luna, “Control of grid-connected power converters based on a virtual admittance control loop,” in Proc. Eur. Conf. Power Electron. Appl., 2013, pp. 1–10.

[9] J. Driesen and K. Visscher, ‘‘Virtual synchronous generators,’’ in Proc. IEEE Power Energy Soc. Gen. Meeting-Convers. Del. Electr. Energy 21st Century, Jul. 2008, pp. 1–3.

[10] Grid Converters for Photovoltaic and Wind Power Systems © 2011 John Wiley & Sons, Ltd

[11] W. Zhang, A. M. Cantarellas, J. Rocabert, A. Luna, and P. Rodriguez, "Synchronous Power Controller With Flexible Droop Characteristics for Renewable Power Generation Systems," in IEEE Transactions on Sustainable Energy, vol. 7, no. 4, pp. 1572-1582, Oct. 2016, doi: 10.1109/TSTE.2016.2565059.

[12] M. Dursun and M. K. DÖŞOĞLU, "LCL Filter Design for Grid Connected Three-Phase Inverter," 2018 2nd International Symposium on Multidisciplinary Studies and Innovative Technologies (ISMSIT), Ankara, Turkey, 2018, pp. 1-4, doi: 10.1109/ISMSIT.2018.8567054.